# An experimental study of turbulence in a density-stratified shear flow

By C. A. G. WEBSTER

Mechanics of Fluids Department, University of Manchester†

(Received 6 August 1963)

This paper concerns an investigation of turbulence in the density stratified shear flow of a specially designed wind tunnel in which the density gradient is created by differential heating of the air. The first three sections of the paper consist of a description of the apparatus and of the mean temperature and velocity gradients in the tunnel, together with a discussion of a method of measuring low wind speeds based on the periodic shedding of vortices by a circular cylinder. In the remaining sections details of the experimentally determined structure of the turbulence of the flow and of its eddy conductivity and viscosity are presented and their dependence on the over-all gradient form of Richardson number, $[g\,\partial T/\partial z]/[T(\partial U/\partial z)^2]$, considered.

## 1. Introduction

Homogeneous isotropic turbulence has received most of the theoretical and experimental attention devoted to the subject of turbulent flows generally, largely because the former problem seems, more than any other, to be sufficiently simple to offer some hope that solutions may be found in any given case. The flows encountered in real life are seldom either homogeneous or isotropic and often have the added complication of a velocity gradient, together with gradients of density, salinity, temperature, etc. These gradients in turn bring about profound changes in the structure of the turbulence.

Two alternatives are open to the would-be experimenter in this field; he may either explore the naturally occurring density stratified flows, such as those in the atmosphere, or he can attempt to reproduce similar conditions in the laboratory. The second of these two courses was chosen for the present investigation and a special wind tunnel, in which essentially linear temperature and velocity gradients extend over an appreciable depth of the flow, was constructed at the Barton Mechanics of Fluids Laboratory of the University of Manchester.‡

This is not the first wind tunnel built for the study of turbulence in a density gradient, cf. Prandtl & Reichardt (1934), but it is unusual, if not unique, in the way grids are used to introduce the temperature and velocity gradients into the flow.

† Now at Nottingham and District Technical College.

‡ Now removed to the Department of Aeronautics, Imperial College, London.

## 2. The wind tunnel

The heated shear-flow wind tunnel, an elevation of which is shown in figure 1, is a small tunnel, nominally 0·5 m square in section. It is of the open-circuit type, being simply constructed of plywood and standing on a 'Dexion' framework. Air first enters the tunnel through a small entry flare, over the mouth of which is stretched a piece of finely knitted nylon fabric. This nylon acts as a very efficient dust trap so that when experiments are performed on reasonably clear days it is possible to operate hot-wire anemometers in the tunnel for quite long periods without them becoming significantly contaminated. Downstream of the nylon the air passes through two wire gauzes, which help to break up any large eddies which may enter the tunnel, and then through the two grids which are the heart of the apparatus and which render it unique.

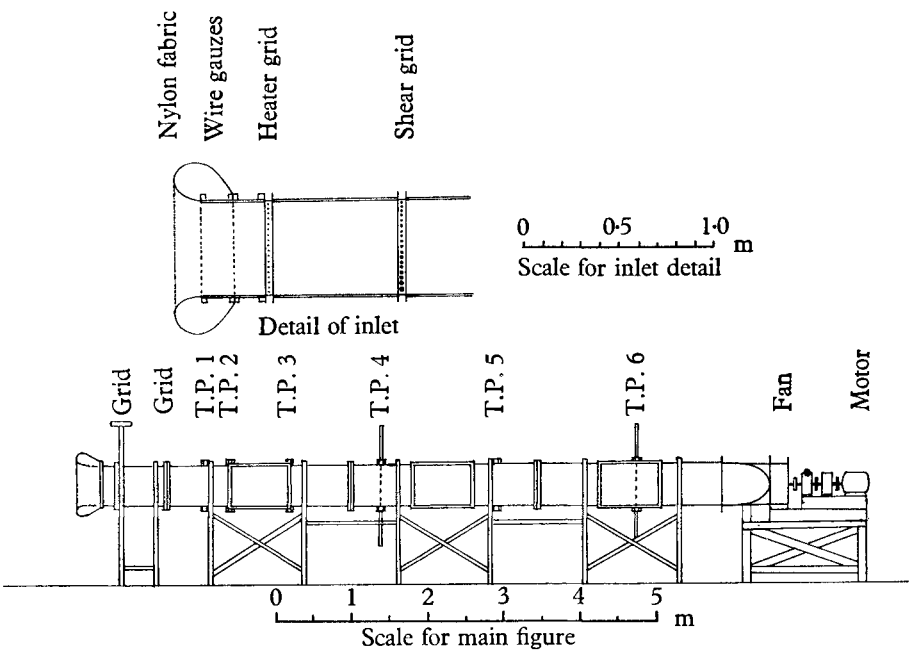


FIGURE 1. Elevation of the wind-tunnel showing the positions of the two special grids and the locations of the traverse points (T.P.).

The first, or heater, grid, which imparts a temperature gradient to the flow, has eighteen horizontal bars consisting of nichrome tube heating elements each 7·9 mm in diameter fixed one above the other at 28 mm centres. The heating elements are connected in a network together with control resistors so that there is a linear gradient of power input across the grid, the greatest power going into the uppermost rod and the least into the lowest, the total power consumption being about 6 kW at 245 V. A range of temperature gradients can be obtained at any particular air speed by the use of a dimmer placed in series with the heater/control resistor complex.

A further 0·6 m downstream the tunnel is spanned by the second, or shear, grid. This grid is similar in appearance to the heater but had seventeen bars as

originally built. The design follows the principles laid down by Owen & Zienkiewicz (1957), the grid finally adopted for use producing a flow with a shear parameter of 0·85 ($= \lambda h/U$ in the terminology of Owen & Zienkiewicz) so that the theoretical variation of velocity with height is given by the formula

$$U(z) = U_{cl}[1 + 0{\cdot}85(z/h - \tfrac{1}{2})], \tag{2.1}$$

where $U(z)$ is the velocity at height $z$ measured from the tunnel floor, $U_{cl}$ is the centre-line velocity and $h$ the height of the tunnel ($= 0{\cdot}51$ m in this case). The necessary variation of drag coefficient is accomplished mainly by reducing the diameter of the bars towards the top of the grid. Since the bars were made from material of commercially available stock sizes it was not always possible for them to have the calculated diameter and some small adjustments were therefore made to their separations so as to preserve the required gradation of drag coefficient.

On testing the grid after installation the anticipated linear velocity profile was not observed over the whole depth of the flow but, on the contrary, the velocities in the lower half of the tunnel became progressively more and more in excess of those predicted. It was, however, possible to correct this defect by an empirical adjustment of the drag of the lower part of the grid so that the whole of the velocity profile became sensibly linear. It is not at all surprising that the first-order theory of Owen & Zienkiewicz, neglecting as it does squares and higher powers of $\lambda h/U$, should fail to provide completely accurate design data for a grid having a shear parameter of 0·85 and it is in fact more remarkable that the resulting profile was largely as desired. By taking into account higher powers of $\lambda h/U$, Ellison† has developed a more refined theory which predicts discrepancies of the type observed.

The working section of the wind tunnel is unremarkable, except insofar as it constitutes some 70 % of the total length of the tunnel. Variation of the over-all velocity of the flow is achieved by adjusting the speed of rotation of the fan, the latter being driven by an a.c. electric motor with a continuously variable gear box.

The centre-line time-mean velocities used in the experiments to be discussed later ranged from 0·4 to 2 m sec$^{-1}$, typical velocity and temperature profiles being shown in figures 2 and 3. These profiles were taken at a station 4·57 m downstream of the shear grid and from them it can be seen that the velocity and temperature gradients are both very nearly linear over an appreciable portion of the flow. From the gradients obtained with maximum power input to the heater grid a graph, figure 4, can be drawn which shows the greatest value of gradient-form Richardson number

$$Ri = \frac{g}{T}\frac{\partial T/\partial z}{(\partial U/\partial z)^2}$$

(where $g$ = the acceleration due to gravity, $T$ = the time-mean temperature in °K, $U$ = the time-mean centre-line velocity and $z$ = the vertical co-ordinate)

† Private communication.

which can be obtained at any particular centre-line velocity, though smaller values can, of course, be obtained at any velocity by reducing the power input to the heater.

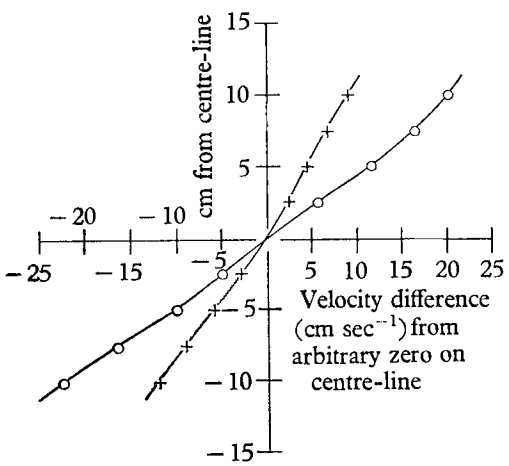


FIGURE 2

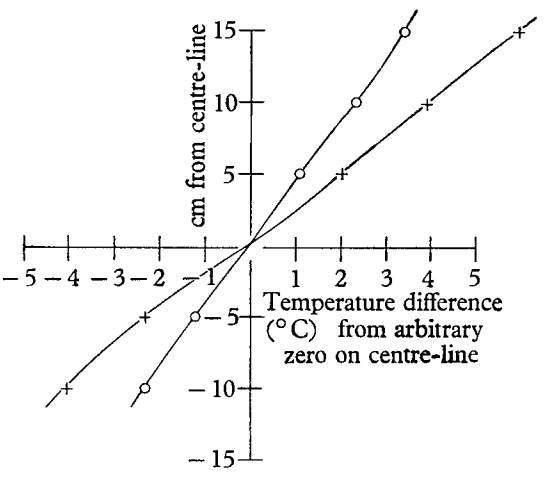


FIGURE 3

FIGURE 2. Typical velocity profiles in the neighbourhood of the centre-line of the wind-tunnel. ○, centre-line velocity = 117 cm/sec; +, centre-line velocity = 55 cm/sec.

FIGURE 3. Typical temperature profiles in the neighbourhood of the centre-line of the wind tunnel. ○, centre-line velocity = 120 cm/sec; +, centre-line velocity = 61 cm/sec.

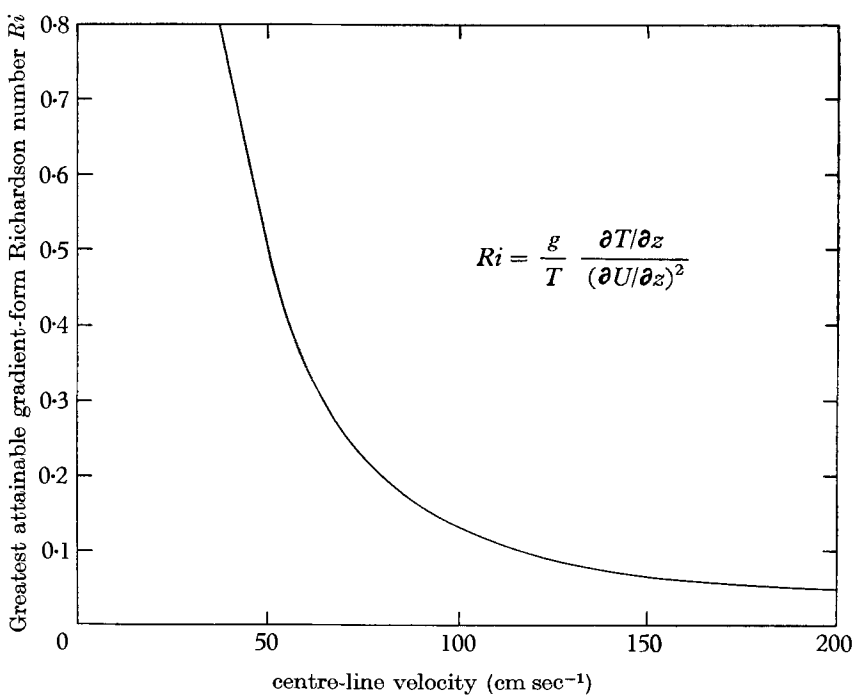


FIGURE 4. Graph showing the maximum-gradient-form Richardson number $Ri$, which can be obtained for any given time-mean centre-line velocity.

## 3. Measurement of mean velocity

Whilst the measurement of mean temperatures and temperature gradients was carried out in a conventional manner using thermometers and thermocouples, a more unusual approach was necessary in the case of velocity determinations. Fluid velocities may be determined, in principle, by measuring any quantity which varies with velocity but the choice is almost always limited to total and static pressure differences although occasionally other phenomena, such as the rate of heat transfer from a heated object, may be used. The routine determination of air-stream velocities in the range 0·4–2·0 m sec$^{-1}$ is not easy when the conventional methods based on pressure measurements are used and the lowest speed which can be measured with reasonable accuracy using robust, easily handled, manometers is probably of the order of 4 m/sec$^{-1}$ corresponding to a pressure difference of about 10 Newton m$^{-2}$ or 1 mm of water. The Pitot-static pressure differences $\frac{1}{2}\rho U^2$ for the range of velocities encountered in the heated shear-flow tunnel are much smaller than this, from 0·1 to 2·5 Newton m$^{-2}$ or 0·01 to 0·25 mm of water. Having decided against conventional pressure measurements some alternative velocity measuring device had to be found. One obvious possibility was to use a hot-wire anemometer but this was also rejected since the calibration of a wire was hardly likely to remain steady enough when exposed to the atmosphere in an open-circuit tunnel.

Another phenomenon, which is strongly dependent on fluid velocity, and about which a large amount of data exists, is the periodic shedding of vortices downstream and to either side of a circular cylinder. The earliest detailed study of this phenomenon was that by Strouhal (1878) in whose honour the non-dimensional group $nd^2/\nu$ (where $n$ is the vortex shedding frequency, $d$ the cylinder diameter and $\nu$ the kinematic viscosity) is known as the Strouhal number $S$. A year later Rayleigh (1879) showed that the Strouhal number should be independent of the elastic properties of the wire and be a function of the Reynolds number only.

The most comprehensive recent sets of experimental observations of the rate of vortex shedding as a function of Reynolds number are those of Roshko (1953), Tritton (1959) and Berger (1962). Each author worked at velocities higher than those of the heated shear-flow tunnel and with very 'quiet' flows having little turbulence; for example, Roshko quotes a level of turbulence of 0·03 % or $\overline{u'^2}/U^2 \approx 10^{-7}$, as opposed to perhaps $10^{-3}$ in the Shear-Flow Tunnel. The curves corresponding to the empirical equations of each author are reproduced in figure 5 in which the Strouhal number $S$ is plotted against the Reynolds number $Re$ of the vortex shedding cylinder. The curves from each source for the range $50 < Re < 150$ are seen to be broadly similar but by no means identical, those of Tritton, who discovered the discontinuity in the range, and Berger, being perhaps the more reliable. The wakes observed at these low Reynolds numbers were laminar with steady shedding frequencies which were detected with hot-wire anemometers and determined from Lissajou figures. Tritton and Berger give no details of observations at Reynolds numbers in excess of 150 and 160, respectively; Roshko, however, continued his measurements up to values of several thousands. Above $Re = 300$ the wake was found to be turbulent

but a predominant frequency could still be detected quite easily. The range $150 < Re < 300$ was concluded by Roshko to be a transition region in which the regular signal from the hot wire was interrupted with bursts of turbulence and in which he was unable to determine any frequency with accuracy. The measurements were made at a distance of six diameters downstream of the cylinder.

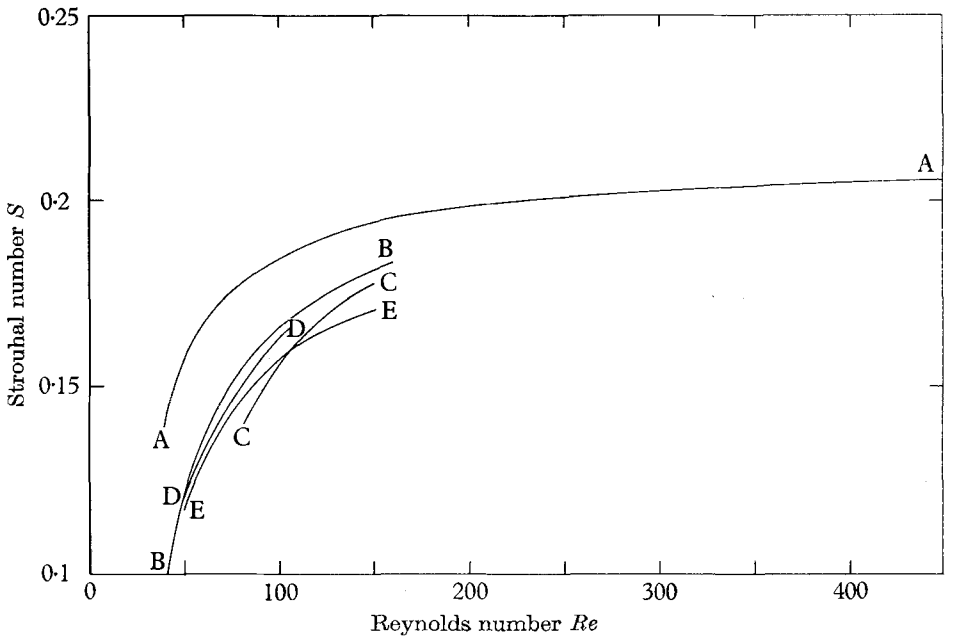


FIGURE 5. Graph showing the variation of Strouhal number, $S$, with Reynolds number, $Re$, as found by various workers. Turbulence-free incident streams: A–A, Roshko $300 < Re$ and present curve for turbulent incident stream; B–B, Roshko $40 < Re < 160$; C–C Tritton $80 < Re < 150$; D–D, Tritton $50 < Re < 105$; E–E, Berger $50 < Re < 150$.

The shedding of vortices by a cylinder thus provides a possible means of measuring fluid velocity and it becomes necessary to design an instrument based on this phenomenon which is easy to make and convenient to use. The rather static arrangements of either wires or rods spanning the tunnel such as were employed by the workers to whom reference has been made are not very suitable for routine use and an alternative device, sketched in figure 6 was adopted. This 'Strouhal Device' consists of a vortex-shedding cylinder attached by a Y-shaped support to a cylindrical holder which also carries a hot-wire anemometer to detect the eddies in the cylinder's wake. The anemometer is arranged so that the hot wire lies about one cylinder diameter behind and at right angles to the main cylinder, this orientation being chosen so that the interference of the hot wire with the vortex shedding process should be a minimum. The details of the effect of one cylinder on the vortex shedding of a second seems to be unknown but it is not unreasonable to suppose that a hot wire parallel to the main cylinder is more likely to have a detrimental effect than one at right angles. The actual sensitive element of the hot-wire anemometer is adjusted to

lie about one cylinder diameter downstream and a little to one side of the main cylinder itself, this adjustment being quite critical if the instrument is to work well. A position too far from the central plane of the wake giving a well-formed but weak signal, while one too near the centre may lead to the detection of both rows of vortices and result in spuriously high values being obtained for the rate of vortex shedding.

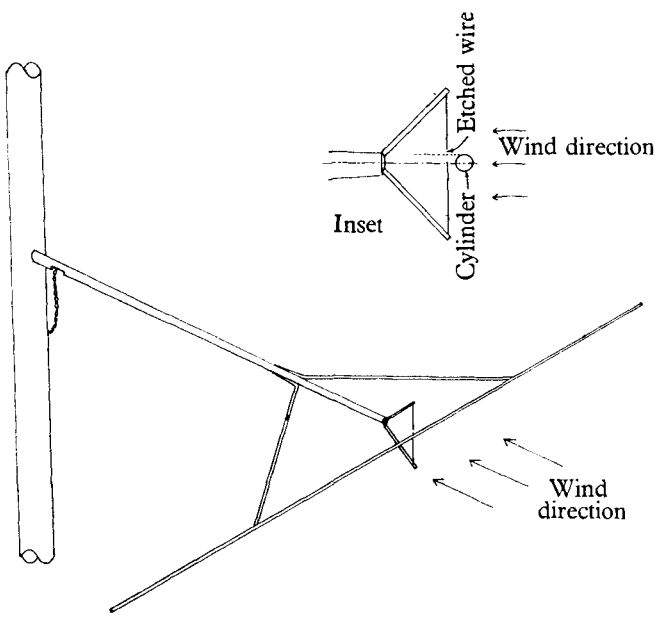


FIGURE 6. Sketch of a velocity-measuring device based on the vortex shedding of a circular cylinder.

If an instrument such as that described above is employed to measure velocities in quiet flows which are relatively free from turbulence it may be found sufficient to determine the frequency at which vortices pass the anemometer by forming Lissajou figures on an oscilloscope, using the amplified hot-wire output signal and a sine-wave oscillator. When, on the other hand, the time-mean velocity of a turbulent stream is to be determined the regular signal due to the vortices has random fluctuations superimposed upon it which render Lissajou figures unsteady. Generally, rates of vortex shedding are appreciably higher than the frequencies associated with the eddies which carry most of the energy of the turbulence in the shear-flow tunnel where the devices were used. In consequence it was found possible to improve the signal-to-noise ratio by passing the hot-wire bridge output through a high-pass filter. This signal was then used to trigger a bi-stable circuit, the square wave output of which was counted over a period of some seconds to obtain a time-mean value of the shedding frequency.

As previously mentioned, Roshko, Tritton and Berger found regular laminar vortex wakes from $Re \approx 150$ down to $Re \approx 50$ and Roshko reported a similar, but turbulent, wake with a well-defined predominent shedding frequency for

$300 > Re$ and with an unsteady intermediate range $150 < Re < 300$. These experiments were carried out in an air stream with a very low level of turbulence, $\overline{u'^2}/U^2 \approx 10^{-7}$. The evidence from work in the turbulent stream of the heated shear-flow wind tunnel, for which $\overline{u'^2}/U^2 \approx 10^{-3}$, shows that this picture must be modified for vortex shedding in the presence of turbulence. Since any of the published empirical formulae lead to roughly the same Reynolds number for a given Strouhal number, irrespective of whether the flow is turbulent or laminar, an approximate value of Reynolds number may be obtained without any decision as to the particular mode of vortex shedding actually in operation. Thus it can be said that in the heated shear-flow wind tunnel, for Reynolds numbers in excess of 90, good signals are obtained which are free from 'missing', that is signals of which no cycles are omitted from the roughly sinusoidal component due to the vortices. At higher Reynolds numbers the signal remains excellent and, if anything, the frequency becomes more stable—this applies all the way through Roshko's 'irregular region' and on to the highest Reynolds numbers recorded ($\approx 550$) without any apparent transitions. At the other end of the scale things are different. Below $Re \approx 80$ the signal deteriorates, taking on an appearance similar to that shown by Roshko for $Re = 180$.

Originally velocities were deduced from Strouhal frequency measurements by the application of Tritton's results, extrapolating his curve for $80 < Re < 150$ given by the equation

$$S = 0{\cdot}224(1 - 29{\cdot}9/Re) \tag{3.1}$$

to higher Reynolds numbers as required. Doubts first began to fall on this method when anomalies were noticed in the velocities obtained for the same fan speed setting, with different diameter cylinders, which seemed to be too large to be attributed to actual velocity differences. An experiment was therefore carried out with pairs of Strouhal devices to try to elucidate the cause of these apparent velocity differences. Two instruments could be placed quickly, one after the other, at the same position in the unheated wind tunnel and mean frequencies were obtained for each device over a number of cycles of interchanges and for a wide range of settings of the gear controlling the tunnel fan speed. The diameters of the cylinders of the two instruments were chosen to be as different as possible consistent with both being able to work in a satisfactory manner over a reasonably wide, common, range of wind speeds, This compromise resulted in cylinder diameters being generally in a ratio of three or four to one, with the smaller cylinder having a diameter between 0·3 and 1 mm. Using Tritton's curves, extrapolated as necessary, graphs were drawn for each cylinder in which mean centre-line velocity was plotted against fan gear setting. A typical plot is shown in figure 7. The two curves do not coincide, the velocities derived from the thicker cylinder being significantly less than those from the thinner one and, if the data is further used to extend Tritton's curves to fill the gap $150 < Re < 300$, the resulting graph does not approach at all well that of Roshko for $Re > 300$. If, however, velocities are recalculated on the basis of Roshko's empirical equation for $Re > 300$ all the data fit together quite smoothly, as shown in the typical graph, figure 8. Under the conditions of the experiment values of Strouhal number, corresponding to low Reynolds number, are found to

be in excess of those previously reported for turbulence-free incident streams but fit Roshko's empirical formula for $Re > 300$, viz.

$$S = 0{\cdot}212(1 - 12{\cdot}7/Re). \tag{3.2}$$

This increase, in the presence of turbulence, of the rate of vortex shedding for a given stream velocity is in accordance with intuition. The firmness with which a developing vortex is attached to its parent cylinder presumably decreases with growth so that at some stage it finally breaks away, thus it is not unreasonable to suppose that the agitation of the vortex by the turbulence will shake it free sooner than in a laminar flow, so allowing the next vortex to begin to form earlier and leading to an increase in the shedding frequency.

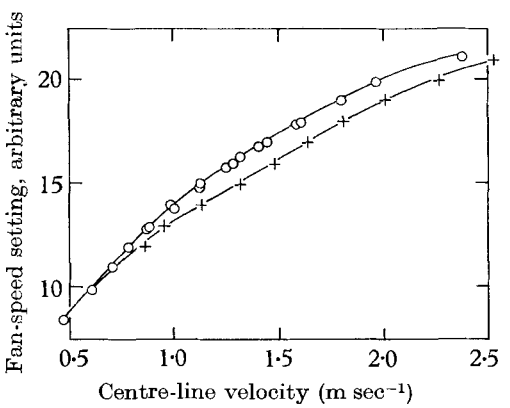


FIGURE 7. Time-mean centre-line velocities, calculated using Tritton's formulae, for two velocity-measuring devices having cylinders of different diameter.

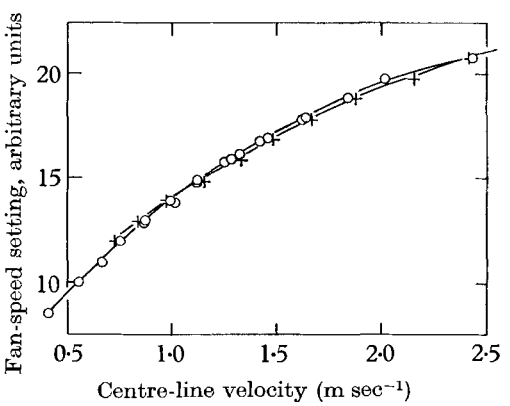


FIGURE 8. Time-mean centre-line velocities, calculated using Roshko's formula, for two velocity-measuring devices having cylinders of different diameter.

To summarize, it may be said that the periodic shedding of vortices by a cylinder can form the basis of a useful and practical means of measuring air-stream velocities down to a few tenths of a metre per second. When working in effectively turbulence-free streams the equations of Tritton and Berger are appropriate in connecting rate of vortex shedding with velocity, whilst if the flow has an appreciable level of turbulence Roshko's 'turbulent wake' equation, equation (3.2) above, can be used at all Reynolds numbers for which a well defined vortex frequency exists. The details of what happens at turbulence intensities between $\overline{u'^2}/U^2 \approx 10^{-7}$ and $10^{-3}$ seem to be as yet unexplored, although it is clear that some sort of transition must occur between the two modes represented by the turbulent and laminar wake forms of the empirical equation connecting Strouhal number with Reynolds number.

## 4. Theories of turbulence in density-stratified flows

For a theoretical background to the experimentally observed and mathematically derived results given later one may turn to the work of Ellison (1957) and Townsend (1958) on turbulence in density stratified flows. Both theories start from the Navier–Stokes equations and the equations of continuity and

heat transfer, but differ somewhat in the devices used to make progress from these. At high Reynolds numbers the rates of dissipation of turbulence are determined mainly by the typical length and velocity scales of the energy-containing eddies, the viscosity playing only a secondary role.

With the instantaneous values of the various quantities which go to make up the field of turbulence expressed in the conventional manner as a time-mean part, denoted by a bar ($^-$), plus a fluctuating part, denoted by a prime ($'$), so that, for example, the stream-wise component $u$ of the flow velocity is expressed as

$$u = \bar{u} + u', \quad \text{where} \quad \overline{u'} = 0, \tag{4.1}$$

Ellison introduced decay times $T_1$, $T_2$ and $T_3$, for $\overline{\rho'^2}$, $\overline{q'^2} = \overline{u'^2} + \overline{v'^2} + \overline{w'^2}$ and $\overline{w'\rho'}$, where $\rho$ is density and $u, v$ and $w$ are the stream-wise, lateral and vertical components of the velocity respectively. These decay times were chosen so that if the production of turbulence were to cease the mixing process would begin to destroy the quantities $\overline{\rho'^2}$, etc., at rates $1/T_1$, etc.; $T_1$, $T_2$ and $T_3$ are then defined by the equations

$$0 = \frac{\overline{\rho'^2}}{2T_1} + \overline{w'\rho'}\frac{\partial\bar{\rho}}{\partial z}, \tag{4.2}$$

$$0 = \frac{\overline{q'^2}}{2T_2} + \overline{u'w'}\frac{\partial U}{\partial z} + \frac{\overline{w'\rho'}g}{\bar{\rho}}, \tag{4.3}$$

$$0 = \frac{\overline{w'\rho'}}{T_3} + \overline{w'^2}\frac{\partial\bar{\rho}}{\partial z} + \frac{\overline{\rho'^2}g}{\bar{\rho}}. \tag{4.4}$$

The equations (4.2), (4.3), (4.4) may now be rearranged to express various quantities such as $K_h/K_m$ (i.e. the ratio of eddy conductivity for heat to the eddy conductivity for momentum) and the $w'\rho'$-correlation in terms of the components of the turbulent energy, the ratio of the decay times and a non-dimensional parameter (such as the flux Richardson number $Rf$, defined as the ratio of the rate at which buoyancy forces extract energy from the turbulence to the rate at which it is supplied by the shear-stress) which provides a measure of the stability of the flow. Thus, for example,

$$\frac{K_h}{K_m} = \frac{\overline{q'^2}\overline{w'^2}[1 - Rf(1 + T_1\overline{q'^2}/T_2\overline{w'^2})]}{2(\overline{u'w'})^2(T_2/T_3)(1 - Rf)^2}. \tag{4.5}$$

If it is supposed that the ratio $T_1/T_2$ is unity, as argued by Ellison, and that under conditions of high stability the turbulence becomes significantly flattened so that $\overline{q'^2}/\overline{w^2} \approx 6$, equation (4.5) indicates that $K_h/K_m$ should fall to zero at a value of $Rf = 0{\cdot}15$, that is to say there exists a critical flux Richardson number $Rf_{\text{crit}}$ which is much less than unity. This point will be taken up again when discussing the experimental results.

Ellison also introduced two length scales, namely $L_M$ defined as $T_2(\overline{q'^2})^{\frac{1}{2}}$ and $L_H$ defined as $(\overline{\rho'^2})^{\frac{1}{2}}/(\partial\bar{\rho}/\partial z)$. The first of these cannot be estimated with any accuracy from the data to be presented. $L_H$, which is representative of the distance travelled by particles before either returning towards their equilibrium level or mixing, can, on the other hand, be obtained with some precision (see

section dealing with figure 15). A further prediction, which is amenable to comparison with experiment, expresses the variation with stability of the correlation between density fluctuations and the vertical component of the turbulence. This is

$$\frac{\overline{w'\rho'^2}}{\overline{\rho'^2}\overline{w'^2}} = \frac{1-Rf\,[1+T_1\overline{q'^2}/T_2\overline{w'^2}]}{2(T_1/T_3)\,(1-Rf)}. \tag{4.6}$$

Townsend, starting as did Ellison from the basic equations for the intensity of the temperature fluctuation and the kinetic energy of the velocity fluctuations of the turbulence, introduced length scales $L_t$ and $L_u$ where

$$\kappa t'\overline{\nabla^2 t'} = -\tfrac{1}{3}\overline{t'^2}(\overline{w'^2})^{\frac{1}{2}}/L_t$$

and $L_u$ is the corresponding dissipation length-scale for the velocity fluctuations, $t'$ being the fluctuating part of the temperature. These scales are nearly equal to the integral scale of the turbulence in neutral conditions. Ignoring advection and radiation terms and writing $k_t^2 = \overline{w't'}^2/\overline{w'^2}\,\overline{t'^2}$ and $k_u = \overline{u'w'}/\overline{w'^2}$ we obtain for the temperature fluctuation

$$(\overline{t'^2})^{\frac{1}{2}} = 3k_t L_t(\partial T/\partial z) \tag{4.7}$$

(where $T$ is the time mean temperature), by the aid of which it is possible to calculate $L_t$ with some accuracy from the data presented later.

The length scale $L_u$ can be shown to be given by the equation

$$L_u = \frac{1}{k_u}\left(\frac{\overline{w'^2}}{\overline{U^2}}\right)^{\frac{1}{2}} \Big/ \left(\frac{1}{\overline{U}}\frac{\partial U}{\partial z}\right)(1-Rf), \tag{4.8}$$

which provides a means of calculating, albeit only roughly, values of $L_u$ corresponding to the results of the present experiments. $Rf$ may now be expressed in terms of the parameters $k_t$, $k_u$, $L_t$, $L_u$, by the relationship

$$Rf = \tfrac{1}{2}\{1-(1-12Ri\,L_t k_t^2/L_u k_u^2)^{\frac{1}{2}}\}, \tag{4.9}$$

from which it is easily seen that in neutral conditions

$$K_h/K_m = 3\,(L_t k_t^2/L_u k_u^2). \tag{4.10}$$

Comparison of these deductions with the observed experimental results is again deferred until later in the paper.

## 5. The experiments

For a field of turbulence as complex as that in the heated shear-flow wind tunnel there are many measurements which could be made and it was necessary to make a choice and concentrate on those which were likely to be of most interest and importance. In addition a degree of selection is also imposed by the use of hot-wire anemometers for taking measurements. For the major part of the experiments the characteristics measured were the streamwise and vertical components of the turbulence together with the temperature fluctuation at the same point, and the three double correlations between them. A few runs were also made in which the horizontal component normal to the flow was measured instead of the vertical component.

For all these measurements a special hot-wire anemometer was used in which a conventional '$X$-wire' was supplemented by a third hot-wire lying close by and parallel to one arm of the $X$, the instrument being operated in the constant current manner.

For a given hot-wire anemometer the rate of heat loss and hence, for a constant heating current, its temperature and electrical resistance depend, *inter alia*, on the velocity and ambient temperature of the incident air stream. Whilst both fluctuations of velocity and temperature will produce changes of the wire resistance which can be detected in the conventional manner, the relative magnitude of the changes of wire resistance produced by them is not constant but depends on the mean wire temperature. A detailed calculation of the sensitivities for a finite wire, taking into account the temperature variation of the parameters involved, has been made by Ellison†. The expressions resulting from these calculations are extremely cumbersome and, though mathematically exact, do not have any immediately obvious physical significance. Thus, though the exact expressions were used in calculating the sensitivities necessary for the reduction of the experimental data to give the results presented later, it is sufficient for the present description of the experimental method to take much simplified equations.

Consider a very long hot-wire anemometer heated by a constant current to a temperature $T_w$ and immersed in a stream of velocity $U$ and ambient temperature $T_a$. Then if $Nu$ is the Nusselt number of the wire, as $T_w \to T_a$

$$\frac{\partial T_w}{\partial U} \to (T_w - T_a)\frac{1}{Nu}\frac{\partial Nu}{\partial U}, \tag{5.1}$$

$$\partial T_w / \partial T_a \to 1, \tag{5.2}$$

while they become comparable for $(T_w - T_a)$ large. Comparing equations (5.1) and (5.2) it can be seen that a hot-wire anemometer becomes relatively more sensitive to temperature than to velocity fluctuations as its mean temperature approaches that of the air and in the limit behaves as a platinum resistance thermometer. A pair of neighbouring hot-wire anemometers operated at widely differing temperatures will, therefore, have different sensitivities to the local fluctuations of velocity and temperature and provide sufficient information for separate values of both to be calculated. For wires such as those used in the heated shear-flow experiment, for which $T_a = 300\,°\mathrm{K}$ and $U = 1$ m/sec may be taken as typical figures, the ratio of the sensitivites to velocity and temperature of the hottest wires at about 500 °K was $-0{\cdot}932$ whereas for a cold wire at 330 °K the ratio became $-0{\cdot}079$.

Briefly then, the experimental procedure made use of three hot-wire anemometers. Two of these constituted the '$X$-wires', familiar from the conventional hot-wire anemometry of unheated turbulence, being operated at relatively high temperatures and thus sensitive to changes in both the velocity and the temperature of their environment. The third wire, lying parallel to one of the former, was much cooler and so responded primarily to temperature fluctuations.

† Private communication.

The total root-mean-square power was obtained for each wire and for the wires taken together in combinations, two or three at a time. From these readings, if taken using vertical wires, and with the computed sensitivities of each wire to velocity and temperature, the root-mean-square power components $\overline{u'^2}$, $\overline{w'^2}$ and the formally similar $\overline{t'^2}$ could be calculated, together with the mean cross-products $\overline{u'w'}$, $\overline{w't'}$ and $\overline{u't'}$. A similar set with $w$ replaced by $v$, was obtained when the wires were mounted horizontally.

From the six main results of each run and a knowledge of the velocity and temperature gradients in the tunnel, further quantities of interest can be deduced, such as the correlation between the various components of the turbulence and the ratio of the eddy conductivity to eddy viscosity. The two major parameters of the main flow upon which these mean properties of the turbulence may be expected to depend are, of course, the flow Reynolds number and the local Richardson number, the latter being defined as $[g\partial T/\partial z]/[T(\partial U/\partial z)^2]$, where $T$ and $U$ are respectively the local time mean temperature and velocity of the flow, $g$ the acceleration due to gravity and $z$ the vertical co-ordinate. In the graphs, which are presented later, the various quantities are plotted against this gradient form of Richardson number, rather than the theoretically more significant flux form, since the latter involves the ratio $K_h/K_m$, the determination of values of which was one of the objects of the study.

The majority of the experimental runs were made at station 5, 4·57 m downstream of the shear grid, a distance corresponding to 174 times the separation between the bars of the grid, but a smaller group was conducted further upstream at station 3, 1·73 m or 66 bar-separations from the grid. In every case the instruments were placed on the centre line of the tunnel. Differences in the results obtained at the two stations show that the flow takes some time to become fully established and the high values of $K_h/K_m$ obtained at station 5 suggest that even there a steady state has not been completely attained. It is unfortunate that the growth of the boundary layers on the tunnel walls so erode the linear velocity profile that it is not possible to retreat appreciably further down the tunnel and away from the grids.

In principle it should be possible to use the tunnel to obtain data over a wide range of Richardson numbers, up to a limiting value set for any given velocity by the total power available, simply by varying the heat input to the grid. In practice it proved difficult to obtain reliable data for combinations of small Richardson numbers and low velocities since, with a reduced power input to the heater grid, temperature fluctuations comparable in magnitude to those generated in the tunnel entered it from the hanger where it was housed. As a consequence runs could not be made having values of Richardson number and velocity chosen as independently as might have been desired and a certain correlation exists between them such that large Richardson numbers tend to be associated with small velocities and vice versa. This correlation is least at intermediate Richardson numbers and over the range $0{\cdot}05 < Ri < 0{\cdot}3$ it proved possible to obtain any desired Richardson number for velocities from 0·5 up to 1·5 m/sec; thus any trend with $Ri$ observed in this range is likely to be fairly reliable.

The accuracy of the results finally obtained is hard to assess, since they are

produced at the end of a very long chain of measurements and calculations, whilst the phenomena under investigation can be themselves only described in statistical terms. The most precisely known quantity is the mean velocity. From the variations of the count during measurement and the reliance placed by Roshko (1953) on his empirical equations, mean velocities are probably known to better than 10 %, in absolute terms, and rather more exactly relatively. The calculated Richardson number, depending as it does on the velocity and temperature gradient, is perhaps accurate to 10 % absolutely and a similar accuracy can reasonably be claimed for the mean curves followed by the turbulence data to be presented.

## 6. The results

In the graphs which follow, data from observations at station 3 are plotted as open rings, whereas those from station 5 are indicated by solid circles; furthermore, on graphs with wind speed as abscissa, points corresponding to conditions in the unheated tunnel are plotted as rings or circles with a 'tail'. Dashed lines, passing through the centre of gravity of clusters of data points, have been drawn on the graphs so as to indicate the general trend of the results. For those graphs with a single curve on which, however, both station 3 and station 5 data are represented the lines are drawn for the latter only.

The three graphs, figures 9, 10 and 11, of $\overline{u'^2}$, $\overline{w'^2}$ and $\overline{v'^2}$, respectively, may be taken together. Comparison of the groups of points taken at stations 3 and 5 and plotted in figures 9 and 10 show that considerable changes occur in the flow between the two positions. All the points, both for $\overline{u'^2}/U^2$ and for $\overline{w'^2}/U^2$ (where $U$ is the time-mean velocity written, for simplicity in place of $\overline{u}$), show a tendency for the ratio to rise with increasing mean velocities, but whereas this rise is quite slight at station 3 showing an increase by a factor of 2 over the range 0·4–1·2 m/sec, at station 5 a strong variation is observed so that from having approximately the station 3 values at a velocity of 0·4 m/sec $\overline{u'^2}/U^2$ and $\overline{w'^2}/U^2$ become eight times greater at 1·2 m/sec. If produced to the left, any reasonable line through the station 5 points would appear to intersect the velocity axis at about 0·3 m/sec.

Although no measurements are available for the $v$-component of the turbulence at station 5, a few horizontal runs were made at station 3. The values of $\overline{v'^2}/U^2$ obtained are plotted in figure 11 and a weak rise with increasing velocity is again observed at a rate comparable with that of the other components at station 3. The possibility of an exchange of energy between the different components can, therefore, be excluded. Neither is the effect strongly dependent on stratification, since the points on the graphs have been plotted irrespective of Richardson number without increasing the scatter above the level of that of the neutral condition points (plotted with 'tails') taken on their own. Thus the origin of this extra energy gained by the turbulence at high velocities is not plain and it is hoped that later work with the apparatus will clear up the mystery.

The next three graphs, figures 12, 13 and 14, may again be considered together. In figure 12 the normalized $w$-component, $\overline{w'^2}/U^2$, is plotted against the (gradient

form) Richardson number while in figure 13 the ratio of $\overline{w'^2}$ to $\overline{u'^2}$ is given. The graph of $\overline{w'^2}/U^2$ shows that this quantity falls off quite spectacularly with increasing Richardson number and it would appear to become effectively zero for $Ri \approx 0{\cdot}45$ and accord well with the idea that vertical motions should be suppressed by the stable stratification of the air.

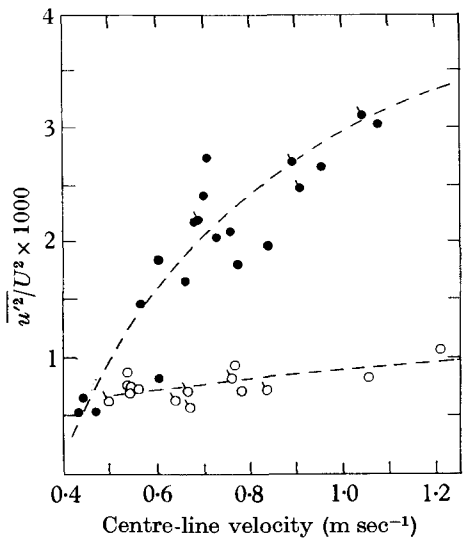


FIGURE 9

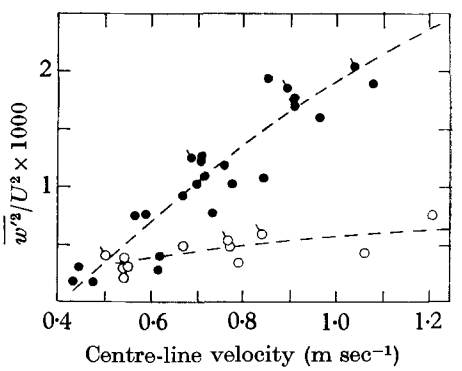


FIGURE 10

FIGURE 9. The mean square of the $u$-component of the turbulence, normalized by dividing by the square of the mean centre-line velocity, plotted against the centre-line velocity. (Points ○ or ● were taken in the unheated wind tunnel.)

FIGURE 10. The mean square of the $w$-component of the turbulence, normalized by dividing by the square of the mean centre-line velocity, plotted against the centre-line velocity. (Points ○ or ● were taken in the unheated wind tunnel.)

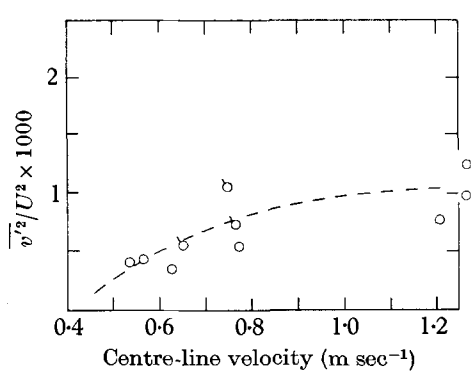


FIGURE 11

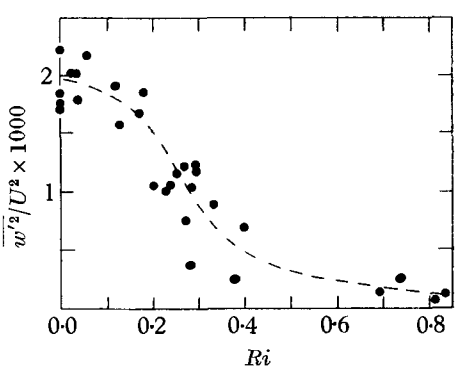


FIGURE 12

FIGURE 11. The mean square of the $v$-component of the turbulence, normalized by dividing by the square of the mean centre-line velocity, plotted against the centre-line velocity, station 3 data only. (Points ○ were taken in the unheated wind tunnel.)

FIGURE 12. The normalized mean-square $w$-component of the turbulence plotted against Richardson number, $Ri$.

In interpreting figure 12 the correlation mentioned earlier between velocity and Richardson number should be borne in mind together with the variation of $\overline{w'^2}/U^2$ with $U$. This effect tends to reduce the slope of the curve and a more conservative estimate of the variation of $\overline{w'^2}/U^2$ with $Ri$ may be had by taking a curve of the same general shape as that in figure 12 but with a slope like that of figure 13. Figure 13, showing the ratio $\overline{w'^2}/\overline{u'^2}$, is probably largely free of velocity effects, which are broadly similar for both $\overline{w'^2}$ and $\overline{u'^2}$. Added support is given to this belief by the excellent manner in which the station 3 points, for which the

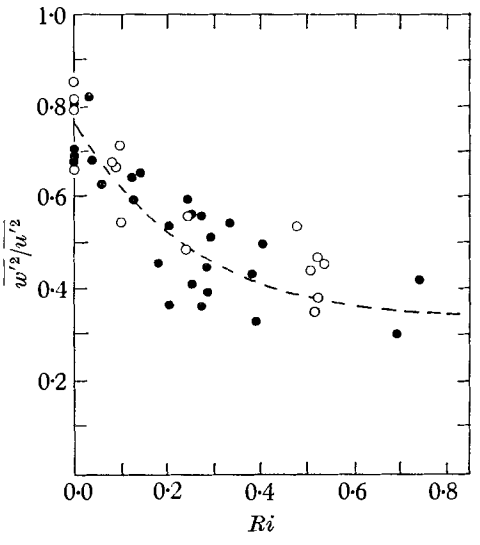


FIGURE 13. The ratio of the mean squares of the $w$- and $u$-components of the turbulence plotted against Richardson number.

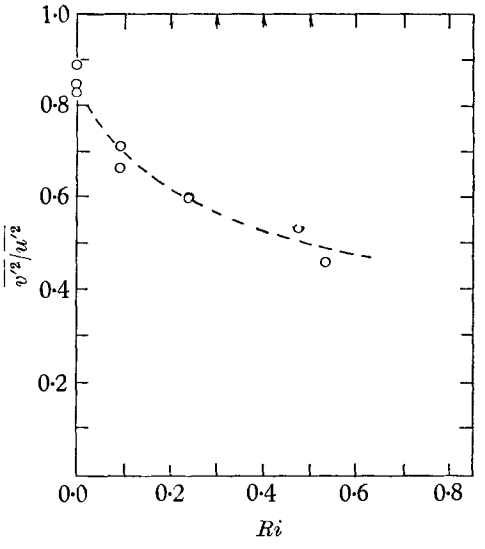


FIGURE 14. The ratio of the mean squares of the $v$- and $u$-components of the turbulence plotted against Richardson number (station 3 data only.)

intensities vary much less with velocity, lie amongst those of station 5. Because of its relative independence of velocity the way in which this curve varies with Richardson number is probably a fairer representation of the form of variation of $\overline{w'^2}$ than that shown in figure 12 and, rather than suggesting a cut off, indicates a more gentle fall to a value in the most stable conditions observed equal to about half that under neutral conditions.

Figure 13 can also help to provide information about the ratio

$$(\overline{u'^2}+\overline{v'^2}+\overline{w'^2})/\overline{w'^2} = \overline{q'^2}/\overline{w'^2},$$

which appears in Ellison's theory and which is important in predicting the value of the critical-flux-form Richardson number and the shape of the curves for $K_h/K_m$ and the other functions. Here we are handicapped by not having much data for $\overline{v'^2}$. However, writing the expression in the form

$$\overline{q'^2}/\overline{w'^2} = \overline{u'^2}/\overline{w'^2}(1+p)+1, \quad \text{where} \quad p = \overline{v'^2}/\overline{u'^2}, \tag{6.1}$$

we see that the answer is not too critically dependent on the value of $\overline{v'^2}$, with a given error in $p$ leading to differences only one third as great in the answer.

Thus no large error will be committed if, in the absence of anything better, we take the value of $p$ from the station 3 data presented in figure 14. Then, from the results of the present experiments, the values set out in table 1 are found with an accuracy of perhaps 10 %. These are rather small compared with the 5·5 used by Ellison though his value was intended to be representative of neutral conditions in the Earth's boundary layer.

If the variations with Richardson number shown in figures 13 and 14, and hence also in table 1, are accepted as being real and not merely reflexions of the velocity dependence of the intensity of the turbulence, then the results indicate changes in the structure of the turbulence which depend on stability. Under neutral conditions the flow is reasonably isotropic with $\overline{u'^2}$ perhaps 10 % in excess of $\overline{v'^2}$ and $\overline{w'^2}$. At higher Richardson numbers both $\overline{v'^2}$ and $\overline{w'^2}$ fall relative to $\overline{u'^2}$, though the effect is more pronounced in the case of $\overline{w'^2}$ which has only $\frac{1}{3}$ its neutral-condition value when $Ri = 0{\cdot}8$. The intuitive notion that turbulence should become 'flat' with a suppression of vertical motions thus seems to be borne out by the observations.

| Richardson number | 0·0 | 0·2 | 0·4 | 0·6 |
|---|---|---|---|---|
| $(\overline{u'^2}+\overline{v'^2}+\overline{w'^2})/\overline{w'^2}$ | 3·4 | 4·1 | 4·7 | 5·0 |

TABLE 1

Figure 15 shows the temperature fluctuations normalized by dividing by the square of the temperature gradient. Despite the fact that the station 3 points (open circles) are rather few in number, it can be seen quite clearly that there are differences between the temperature fluctuations at the two positions. At high Richardson numbers the curve followed by the points obtained at station 5 falls effectively to zero, while at station 3 it still retains an appreciable fraction of the amplitude achieved in neutral conditions, being perhaps three or four times the station 5 value for $Ri = 0{\cdot}4$. Under conditions of less extreme stability the two curves approach one another and become approximately the same below $Ri = 0{\cdot}2$, though the shortage of station 3 points in that region makes it difficult to be completely certain of this.

If it is supposed that the time taken for equilibrium to be reached becomes longer as the stability increases, then the data of figure 15 imply that, whereas at small Richardson numbers equilibrium is attained before reaching station 3, under highly stable conditions insufficient time elapses between the generation of the temperature fluctuations and their arrival at this point. Station 5 is, however, 2·7 times further from the shear grid and 2·3 times from the heater so that correspondingly longer times are available in which the steady state can be reached. Further support is given to this argument in a later discussion of suggested values for the decay times $T_1$, $T_2$ and $T_3$ of Ellison's theory when the decay time $T_1$, associated with temperature fluctuations, is found to increase with stability.

The quantity plotted in figure 15 is equal to $L_H^2$ of Ellison's theory and suggested values of $L_H$ derived from station 5 results are given in table 2. Interpreting

$L_H$ as being a length typical of the vertical distance travelled by particles before either returning towards their equilibrium levels or mixing, these data give further proof of the reduction of the vertical scale of the turbulence in highly stable conditions. Only the roughest of estimates of $L_M$ is possible. Using the

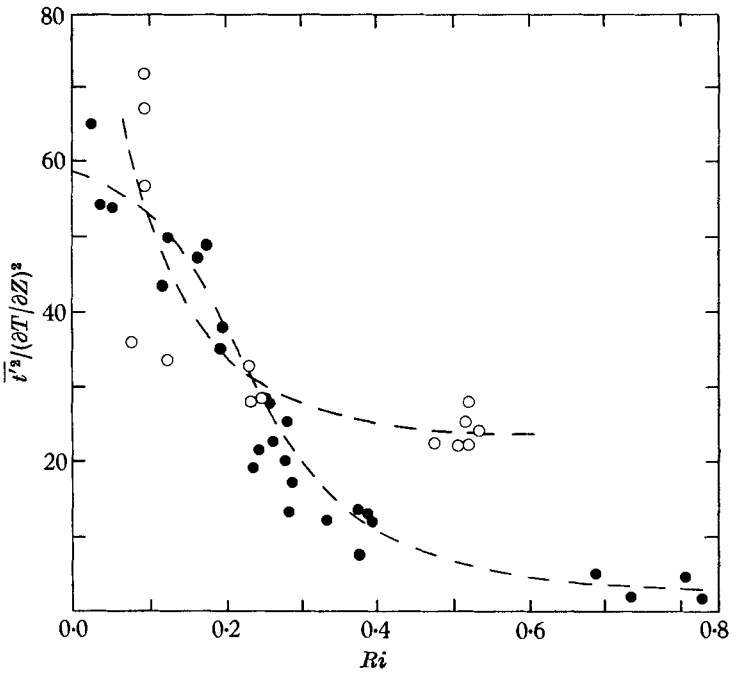


FIGURE 15. The mean square of the temperature fluctuation, normalized by dividing by the square of the vertical gradient of time-mean temperature, plotted against Richardson number.

| Richardson number | 0·0 | 0·2 | 0·3 | 0·4 | 0·6 | 0·8 |
|---|---|---|---|---|---|---|
| Ellison's $L_H$ (mm) | 77 | 62 | 45 | 33 | 21 | 17 |
| Townsend's $L_t$ (mm) | 67 | 63 | 60 | 53 | 39 | 31 |

TABLE 2

various relationships between $L_M$ and the available data, values for neutral conditions may be obtained which range from 0·16 to 0·29 m. The Townsend length scale $L_t$ may be found immediately from $L_H$ by use of the data of the $(w', t')$-correlation graph, figure 16, and values are tabulated in table 2.

The correlations between the components $w'$ and $t'$, $u'$ and $w'$, $u'$ and $t'$ are given in figures 16, 17 and 18, respectively. In general, the points from both stations seem to lie together quite well, but is is probably better that attention should be confined to the station 5 points which correspond to more nearly steady-state conditions. The $(w', t')$-correlation falls rapidly with increasing Richardson number from a value of perhaps 0·38 in neutral conditions to a value around 0·2 for $Ri$ in excess of 0·3. The neutral condition value is high compared with the 0·3 calculated

by Ellison on the basis of $T_1/T_3 = 6$ but accords well with the 0·4 indicated by Swinbank's (1955) results. The shape of the curves agrees broadly with that predicted by equation (4.6) but, taking the observed correlation coefficient, a value $T_1/T_3 = 3{\cdot}5$ is obtained for neutral conditions.

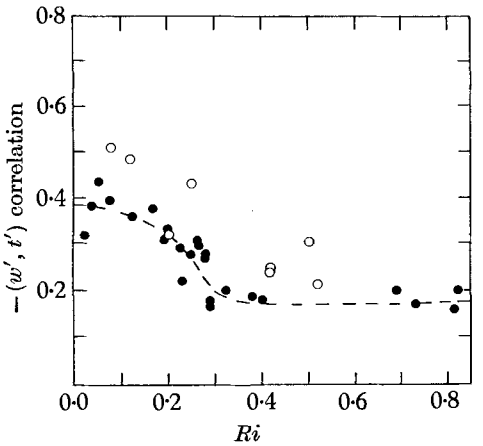


FIGURE 16. $(w', t')$-correlation plotted against Richardson number.

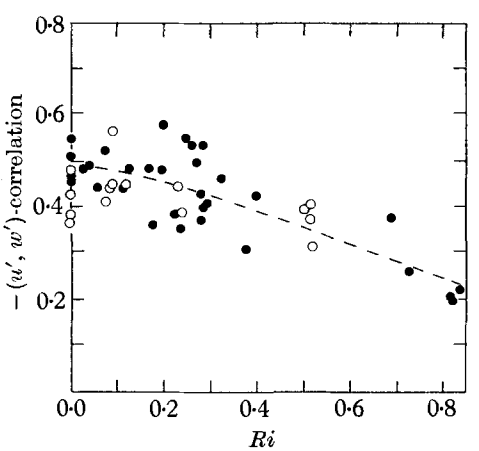


FIGURE 17. $(u', w')$-correlation plotted against Richardson number.

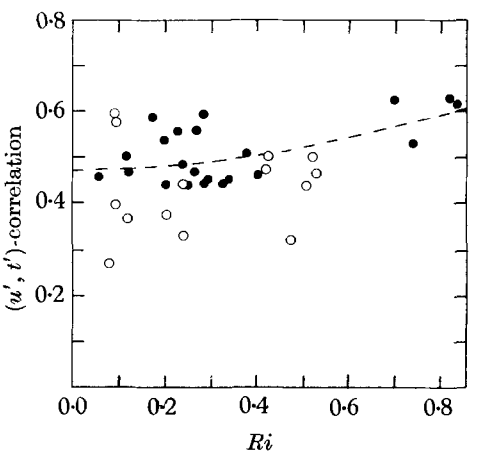


FIGURE 18. $(u', t')$-correlation plotted against Richardson number.

The $(u', w')$-correlation is less strongly dependent on the Richardson number, having a neutral condition value a little less than 0·5, and so is rather in excess of the 0·4 usually taken for this constant. The $(u', t')$-correlation shows a distinct tendency to increase with Richardson number, suggesting that as the vertical transport of temperature by the turbulence is reduced by the stability, horizontal transport becomes more significant. This effect is that which would be anticipated if the turbulence degenerated into a wave-like motion at high Richardson numbers.† Information as to the behaviour of the $(v', t')$-correlation is, unfortunately, too scanty to be able to decide whether this also shows an increase with stability.

† The author is indebted to Dr A. A. Townsend for this observation.

One of the primary aims of the present study was the investigation of the effect of thermal stratification on the turbulent transport processes in the flow. The ratio of the rates of convection by the $w$- and $u$-components of the turbulence, i.e. $\overline{w't'}/\overline{u't'}$, is given in figure 19 and is seen to fall catastrophically from unity in neutral conditions to only about 0·5 at $Ri$ equal to 0·2 and even less for higher Richardson numbers.

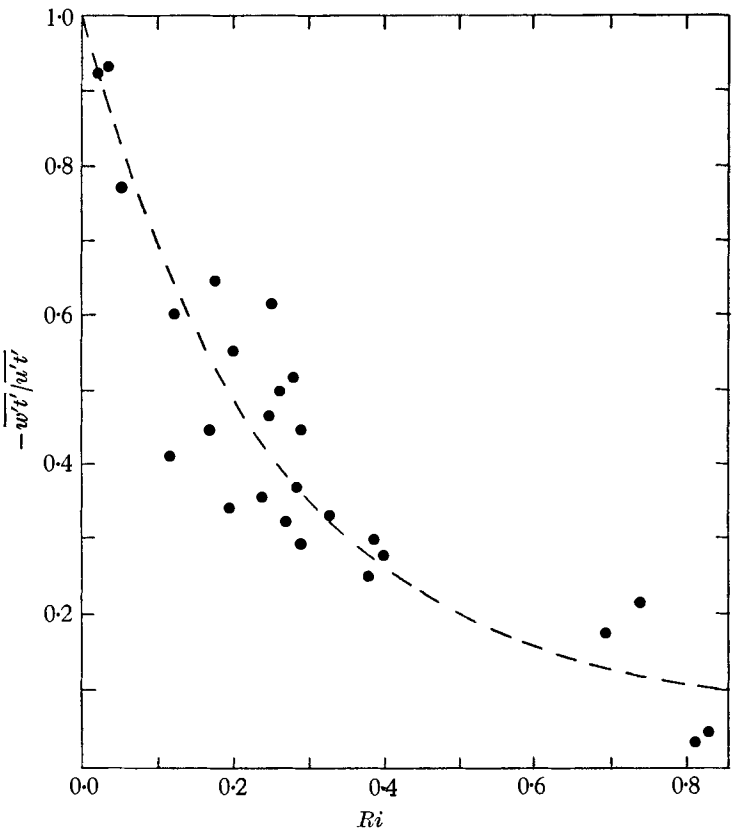


FIGURE 19. The ratio of $\overline{w't'}$ and $\overline{u't'}$ plotted against Richardson number.

Closely related to $\overline{w't'}/\overline{u't'}$, and of fundamental interest, are the eddy conductivity $K_h$ and eddy viscosity $K_m$ together with their ratio $K_h/K_m$. The ratios of $K_h$ to $K_m$ for the two stations are shown in figures 20 and 21; the points on graph 21 having been selected so as to preserve only those in which there can be complete confidence. One is immediately struck by the high values shown.

The values of $K_h/K_m$ obtained by previous workers are very variable, even under neutral conditions (i.e. $Ri = 0$), and suggested values range from 0·8 derived by Swinbank (1955) from meteorological data, to 1·5 by Sherwood & Woertz (1939) for water vapour in a duct, which value is also indicated by Pasquill's (1949) work in the atmosphere. In general the majority of values at fairly low Reynolds numbers seem to cluster around 1·35. Page, Schlinger, Breaux & Sage (1952) obtained 1·30 by using a small duct, with a heated roof and cooled

floor, in which the air velocity was so high as to only give very small Richardson numbers. Later, Schlinger, Berry, Mason & Sage (1953) arrived at 1·35 with the same apparatus. The measurements of Ellison & Turner (1959, 1960) using salt solution in a water channel also indicate values in the range 1·3–1·4.

If there are conflicting views as to the value of $K_h/K_m$ in neutral conditions, its variation with stability is even less well established. The data presented by Swinbank (1955) are too scattered to indicate any more than a general trend but those of Ellison & Turner do show a strong dependence on Richardson number. For very large Richardson numbers, Proudman (1953), working on observations made in the Kattegat, gives $K_h/K_m$ of the order 0·05–0·03 for $Ri$

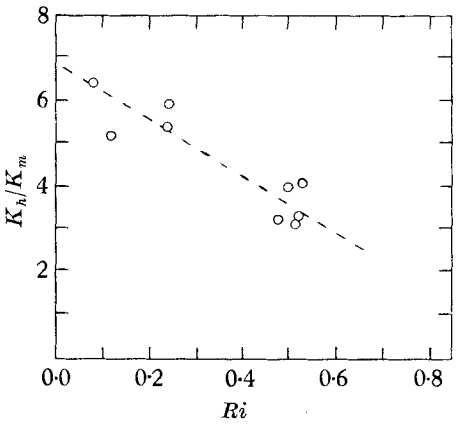


FIGURE 20. The ratio of eddy conductivity to eddy viscosity ($K_h/K_m$) plotted against Richardson number (station 3 data only).

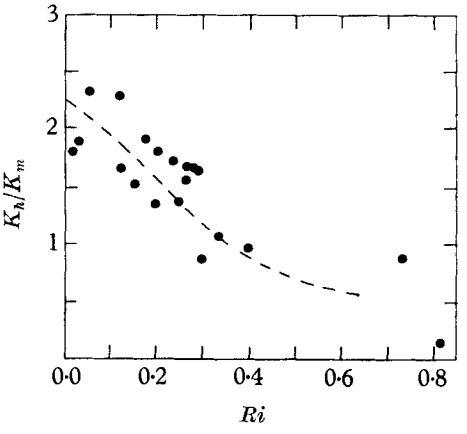


FIGURE 21. The ratio of eddy conductivity to eddy viscosity ($K_h/K_m$) plotted against Richardson number (station 5 data only).

in the range 4–10. Though these values of the ratio are very small, compared with those generally encountered, they are still several orders of magnitude greater than could arise from molecular diffusion. It has been suggested by Stewart (1959) that under these extreme conditions the transfer mechanism is more akin to the breaking of internal waves than to turbulence in the usually accepted sense.

The dependence on stability is clearly seen, in figures 20 and 21, but the absolute values of $K_h/K_m$ are much larger than those previously observed, being specially so in the case of the station 3 points. These discrepancies may be accounted for by postulating that the two transport processes take a finite time to become fully established but that, of the two, the time constant for eddy viscosity, $T_m$ say, is longer than that for eddy conductivity, $T_h$. In figures 22 and 23 the eddy viscosity and conductivity respectively are shown plotted against the Richardson number for the two stations. Whereas the values of $K_h$ are substantially the same at the two positions, $K_m$ is approximately three times as great at station 5 as at station 3 and is presumably still changing at a time when $K_h$ has become established at its final value.

In passing it may be noted that an appropriate length scale for the stretching of eddies by the shear and for the development of $K_m$ is $U/(\partial U/\partial z)$ which has a

value of about 0·5 m in the Shear-Flow Tunnel. Such a length is comparable with the distances between the heater grid and the working stations.

If the $K_h/K_m$ curves, and especially that of figure 21 for which there is the most data, are supposed to be of the correct shape except for being 'stretched' vertically, it is possible to estimate a value for $Rf_{\text{crit}}$, the value of the flux-form Richardson number at which $K_h/K_m$ falls to zero. Taking the formal definition of $Rf$,

$$Rf = Ri(K_h/K_m), \tag{6.2}$$

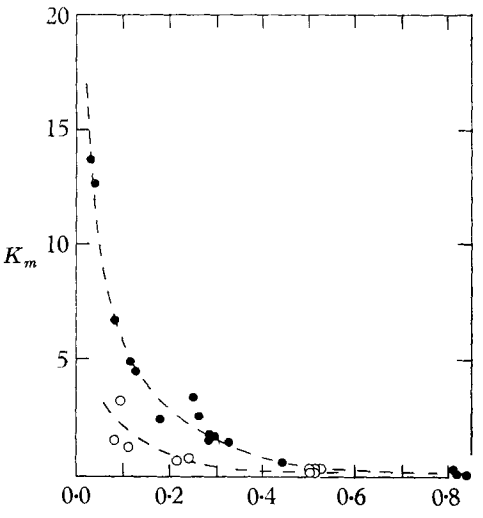


FIGURE 22. The eddy viscosity ($K_m$) plotted against Richardson number.

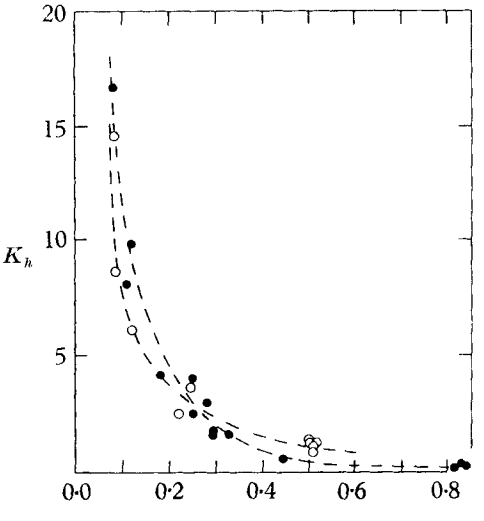


FIGURE 23. The eddy conductivity ($K_h$) plotted against Richardson number.

$Rf_{\text{crit}}$ is then the limit to which the right-hand side of this expression tends as $Ri$ increases. From figure 24 this limit is found to be approximately 0·35. The curve is drawn to pass through the majority of the data. As indicated on the graph, if very large values of $Ri$ are taken, points are obtained which lie to the right of the curve. However, it is reasonable to ignore them for the purposes of calculating $Rf_{\text{crit}}$ and suppose that they are due either to experimental difficulties involved in working at extreme stabilities or to more fundamental causes such as the break-down of normal turbulent transport processes and their replacement by some other mechanism, perhaps of a wave-like nature.

Just as in the case of $K_h/K_m$, our knowledge of $Rf_{\text{crit}}$ generally is again very slight. Ellison calculated a value of 0·15 in his 1957 paper, which was also found from experiment by Ellison & Turner (1959). The work of Proudman mentioned earlier suggests, on the other hand, that $Rf_{\text{crit}}$ may be as great as 0·25 or 0·3. The high values of the critical Richardson number deduced from the results of the present experiments may be attributed to the failure in attaining steady conditions, any estimates made from the station 3 results, where departures from equilibrium are even greater than at station 5, leading to still higher answers.

The experimental data may also be used to make fairly reliable estimates, for the present flow, of the ratio $T_1/T_2$ introduced by Ellison and of the ratios $L_t/L_u$ and $L_t k_t^2/L_u k_u^2$ introduced by Townsend. Estimates of $T_1/T_2$ from equation (4.5) taking $Rf_{\text{crit}} = 0{\cdot}35$ and the values of $\overline{q'^2}/\overline{w'^2}$ from table 1 are set out in

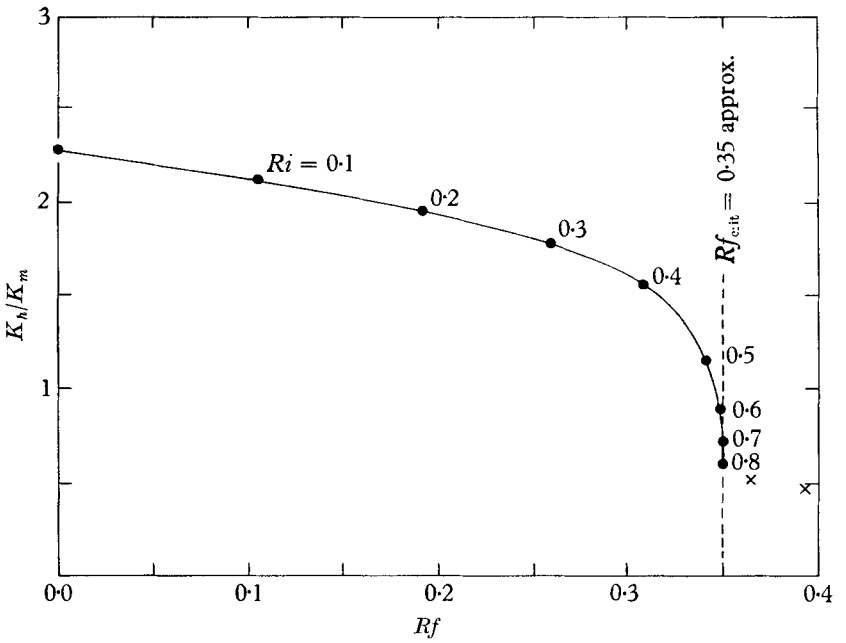


FIGURE 24. The ratio of eddy conductivity to eddy viscosity ($K_h/K_m$) plotted against flux-form Richardson number. A critical value of flux-form Richardson number being indicated in the region of $Rf = 0{\cdot}35$. ×, Ignored points.

| Richardson number | 0·0 | 0·2 | 0·3 | 0·4 | 0·6 |
|---|---|---|---|---|---|
| $T_1/T_2$ | 0·55 | 0·45 | 0·42 | 0·40 | 0·37 |
| $T_1 U$(m) | 1·33 | 3·25 | 3·79 | 4·23 | (3·46) |
| Approx. $T_1$ (sec) | — | 3 | 5 | 7 | — |

TABLE 3

table 3. Equation (4.2) can be rearranged to give $T_1$ in terms of the quantities for which graphs are available,

$$T_1 = \frac{1}{2U} \frac{\overline{t'^2}}{(\partial T/\partial z)^2} \frac{(\partial T/\partial z)}{\overline{w't'}/U}. \tag{6.3}$$

$T_1 U$, the distance travelled by air during the decay time of $\overline{\rho'^2}$ if moving with the centre-line velocity is also tabulated in table 3, together with respresentative values of $T_1$.

The values of the ratio $T_1/T_2$ found above are approximately only half those suggested by Ellison, the differences corresponding largely to the differences in $Rf_{\text{crit}}$. If, as an alternative, it is assumed that $T_1/T_2 = 1$, $Rf_{\text{crit}}$ must take a value 0·2 (taking $\overline{q'^2}/\overline{w'^2} = 5$ for large $Ri$). Such a figure would also be obtained

from figure 21 if the ordinates were 'compressed' to 0·55 of their original values. This process would then lead to $K_h/K_m = 1{\cdot}3$ in neutral conditions so bringing it in line with the estimates of previous workers. There is thus some fairly strong evidence in support of the belief that under equilibriun conditions the critical flux Richardson number has a value of about 0·2 and that $T_1/T_2$ is approximately unity, as supposed by Ellison, the values of 0·35 for the former and around 0·5 obtained for the latter from the present experiments being a further symptom of the developing flow.

We turn now to the quantities that appear in Townsend's theory. Values of $L_t$ and $k_t$ have already been given; if the shear parameter $k_u = \overline{u'w'}/\overline{w'^2}$ is plotted against Richardson number then, despite the scatter, a mean value of 0·6 is indicated, which seems to be independent of the stability of the flow. Rough estimates of $L_u$ may be derived from equation (4.8) and these are set out in table 4, along with the ratios $L_t/L_u$ and $L_t k_t^2/L_u k_u^2$. Reservations must be held as to the

| Richardson number | 0·0 | 0·2 | 0·3 | 0·4 | 0·6 | 0·8 |
|---|---|---|---|---|---|---|
| $L_u$(mm) | 42 | 35 | 26 | 22 | 15 | 12 |
| $L_t/L_u$ | 1·6 | 1·9 | 2·5 | 2·6 | 2·7 | 2·7 |
| $L_t k_t^2/L_u k_u^2$ | 0·90 | 0·38 | 0·33 | 0·21 | 0·19 | 0·19 |

TABLE 4

accuracy of the values of $L_u$ suggested above since the equation involves both $\overline{w'^2}/U^2$ and $Rf$ explicitly. The former, with its dependence on $U$, and the latter involving, as it does, $K_h/K_m$ with its atypically high values, are probably peculiar to the shear-flow wind tunnel rather than characteristics of turbulence generally, so that considerable care must be exercised if the results derived from these quantities are applied in any other situation.

By equation (4.11) a neutral condition value of 2·7 may be predicted for $K_h/K_m$ at station 5, which is not too different from the 2·2 to 2·3 actually observed, especially when the large number of stages involved in the calculations are taken into account.

Perfect agreement between the observations and the theory cannot be anticipated since the data already presented shows that the flow in the tunnel is developing. Only $k_u$, of the four parameters appearing in the theory, seems to be really independent of Richardson number, though $k_t$ and $L_t/L_u$ show signs of becoming constant at high stabilities. Townsend, by contrast, supposed that $k_t$, $k_u$ and $L_t/L_u$ were substantially independent of Richardson number. Thus, since the conditions of the present experiments are only a crude approximation to those specified by Townsend it is not too surprising that the more delicate predictions cannot be confirmed.

## 7. Conclusions

The experiments just described have been both interesting and a little disappointing. Interesting in so far as they have produced much new information concerning the variation with stability of the various quantities associated with turbulence and turbulent transport processes while at the same time indicating

the possibility of a detailed study of these complicated flows. Disappointing in that it was not possible to attain steady-state conditions in which, for example, $K_h/K_m$ had the neutral-condition value found by previous workers; the indications were that a doubling, or even trebling, of the linear dimensions of the apparatus would be necessary to do so. In particular the absolute values of the various results deducted from the experimental data are probably peculiar to the shear-flow wind tunnel, rather than characteristics of turbulence generally, so that considerable care must be exercised if they are applied in another situation.

The manner in which these quantities vary with stability is likely to be more nearly universal. This being the case, the results obtained serve to confirm many of the views previously held. Thus $K_h/K_m$ falls with increasing $Ri$ and there is a sharply defined critical flux Richardson number. The turbulence also appears to become 'flat' with increasing stability, the velocities and the length scales associated with vertical motions becoming less as $Ri$ increases. Less well anticipated is the phenomenon of the long time-constant associated with the development of the flow.

## REFERENCES


Berger, E. 1962 *D.V.L. Rep.*

Ellison, T. H. 1957 *J. Fluid Mech.* **2**, 456.

Ellison, T. H. & Turner, J. S. 1959 *J. Fluid Mech.* **6**, 423.

Ellison, T. H. & Turner, J. S. 1960 *J. Fluid Mech.* **8**, 514.

Owen, P. R. & Zienkiewicz, H. K. 1957 *J. Fluid Mech.* **2**, 521.

Page, F., Schlinger, W. G., Breaux, D. K. & Sage, B. H. 1952 *Ind. Engng Chem.* **44**, 424.

Pasquill, F. 1949 *Proc. Roy. Soc.* A, **198**, 116.

Prandtl, L. & Reichardt, H. 1934 *Dtsche Forschung.* **21**, 110.

Proudman, L. F. 1953 *Dynamical Oceanography.* London: Methuen.

Rayleigh, Lord, 1879 *Phil. Mag.* **7**, 161.

Roshko, A. 1953 *N.A.C.A., TN* 2913.

Schlinger, W. G., Berry, V. J., Mason, J. L. & Sage, B. H. 1953 *Ind. Engng Chem.* **45**, 662.

Sherwood, T. K. & Woertz, B. B. 1939 *Trans. Amer. Inst. Chem. Engrs,* **35**, 517.

Stewart, R. W. 1959 *Advances in Geophysics,* vol. 6, p. 303. New York: Academic Press.

Strouhal, V. 1878 *Ann. Phys. Chem.* **5**, 216.

Swinbank, W. C. 1955 *C.S.I.R.O. Div. Met. Phys., Tech. Pap.* no. 2.

Taylor, G. I. 1931 *Rapports et Procés-Verbaux du Conçeil Permanent International pour l'Exploration de la Mer,* **78**, 35.

Townsend, A. A. 1958 *J. Fluid Mech.* **3**, 361.

Tritton, D. L. 1959 *J. Fluid Mech.* **6**, 547.